Journal of Thrombosis and Haemostasis, **16**: 1153–1163 DOI: 10.1111/jth.14023

ORIGINAL ARTICLE

Extracellular vesicles from human saliva promote hemostasis by delivering coagulant tissue factor to activated platelets

Y. YU,*† E. GOOL,*†‡ R.J. BERCKMANS,*† F.A.W. COUMANS,‡† A.D. BARENDRECHT,§ C. MAAS,§ N. N. VAN DER WEL,¶ P. ALTEVOGT,**†† A. STURK*† and R. NIEUWLAND*†

*Laboratory of Experimental Clinical Chemistry, Academic Medical Centre (AMC) of the University of Amsterdam; †Vesicle Observation Centre, AMC; ‡Department of Biomedical Engineering and Physics, AMC, Amsterdam; §Department of Clinical Chemistry and Haematology, University Medical Center Utrecht, Utrecht; ¶Department of Medical Biology, Electron Microscopy Centre Amsterdam, AMC, Amsterdam, the Netherlands; **Skin Cancer Unit, German Cancer Research Center; and ††Department of Dermatology, Venereology and Allergology, University Medical Center Mannheim, Ruprecht-Karl University of Heidelberg, Heidelberg, Germany*

To cite this article: Yu Y, Gool E, Berckmans RJ, Coumans FAW, Barendrecht AD, Maas C, van der Wel NN, Altevogt P, Sturk A, Nieuwland R. Extracellular vesicles from human saliva promote hemostasis by delivering coagulant tissue factor to activated platelets. *J Thromb Haemost* 2018; **16**: 1153–63.

Essentials

- Human salivary extracellular vesicles (EVs) expose coagulant tissue factor (TF).
- Salivary EVs expose CD24, a ligand of P-selectin.
- CD24 and coagulant TF co-localize on salivary EVs.
- $TF^+/CD24^+$ salivary EVs bind to activated platelets and trigger coagulation.

Summary. *Background:* Extracellular vesicles (EVs) from human saliva expose coagulant tissue factor (TF). Whether such TF-exposing EVs contribute to hemostasis, however, is unknown. Recently, in a mice model, tumor cell-derived EVs were shown to deliver coagulant TF to activated platelets at a site of vascular injury via interaction between P-selectin glycoprotein ligand-1 (PSGL-1) and P-selectin. *Objectives:* We hypothesized that salivary EVs may deliver coagulant TF to activated platelets via interaction with P-selectin. *Methods:* We investigated the presence of two ligands of P-selectin on salivary EVs, PSGL-1 and CD24. *Results:* Salivary EVs expose CD24 but PSGL-1 was not detected. Immune depletion of CD24-exposing EVs completely abolished the TF-dependent coagulant activity of cell-free saliva, showing that coagulant TF and CD24 co-localize on salivary EVs. In a whole blood perfusion model, salivary EVs accumulated at the surface of activated platelets and promoted fibrin generation, which was abolished by an inhibitory antibody against human CD24. *Conclusions:* A subset of EVs in human saliva expose coagulant TF and CD24, a ligand of P-selectin, suggesting that such EVs may facilitate hemostasis at a site of skin injury where the wound is licked in a reflex action.

Keywords: coagulation; extracellular vesicles; P-selectin; saliva; tissue factor.

Correspondence: Yuanjie Yu, Academic Medical Centre of the University of Amsterdam, Department of Clinical Chemistry (Room B1-238), Meibergdreef 9, 1105 AZ Amsterdam, the Netherlands
Tel: +31 205 665 803
E-mail: y.yu@amc.uva.nl

Received: 30 October 2018
Manuscript handled by: W. Ruf
Final decision: P.H. Reitsma, 30 March 2018

Introduction

Extracellular vesicles (EVs) are cell-derived membranous particles present in human body fluids that contribute to coagulation [1,2], immune response [3,4] and tumor progression [5,6], and may provide biomarkers in various diseases [7,8]. Body fluids exposed to the 'milieu extérieur', such as saliva and urine, contain coagulant tissue factor (TF)-exposing vesicles. TF, a transmembrane receptor, binds factor (F) VII and triggers extrinsic coagulation. Under physiological conditions, TF is constitutively expressed and produced by extravascular cells, and this TF will contact the blood upon vascular injury. TF-exposing EVs in saliva most likely provide a source of coagulant TF in addition to the TF already present in the skin, which may explain the reflex of licking a wound. Previously, we demonstrated that saliva shortens the clotting time (CT) of human wound blood *in vitro*, suggesting that salivary EVs may play a role in hemostasis at sites of skin injury as a result of the licking reflex [2].

Blood from healthy humans does not contain EVs exposing coagulant TF. Clearly, the presence of such EVs within the circulation is potentially dangerous, as reflected by the fact that EVs, isolated from a human wound and

exposing coagulant TF, triggered TF-dependent thrombus formation in a rat venous stasis model [9,10]. Under pathological conditions, cancer cells express TF [11,12] and release EVs exposing TF [13], and there is increasing evidence that circulating TF-exposing EVs are associated with the incidence of venous thromboembolism in cancer patients [1,14]. Thomas *et al.* showed in a murine model of vascular injury that tumor cell-derived EVs exposing TF and P-selectin glycoprotein ligand-1 (PSGL-1) adhered to activated platelets by binding to P-selectin. In this manner, coagulant 'blood-borne' TF is deposited and concentrated at a site of vascular injury, where the deposited TF will trigger coagulation [15]. A similar mechanism has been proposed for monocyte-derived EVs ($PSGL\text{-}1^+/TF^+/CD14^+$) in a laser-induced model of endothelial injury [16].

There is a second ligand known for P-selectin, CD24 [17,18]. CD24 was first described in mice by Springer *et al.*, who named this protein 'heat shock antigen' because of the resistance to heat [19]. CD24 consists of a small protein core of 27 amino acids that are heavily glycosylated, and CD24 is bound to the membrane by a phosphatidylinositol anchor [20,21]. In humans, CD24 is exposed by hematopoietic cells, mostly B cells [22] and granulocytes [20,23].

Here we investigate whether coagulant TF-exposing EVs from human saliva expose ligands of P-selectin, and whether such EVs can deliver coagulant TF to activated platelets and trigger coagulation.

Experimental procedures

Materials

For flow cytometry analysis, antibodies against CD8-phycoerythrin (PE; clone SK-1), CD19-PE (clone HIB19), CD56-allophycocyanin (APC; clone TULY56), CD146-PE (clone P1H12) and CD162-PE (P-selectin glycoprotein ligand-1, PSGL-1; clone KPL-1) were obtained from eBioscience (Santa Clara, CA, USA). Anti-CD24-PE (clone SN3), CD61-APC (clone Y2/51), CD66b-fluorescein isothiocyanate (FITC; clone 80H3) and CD326-PE (epithelial cell adhesion molecule, EpCAM; clone EBA-1) were obtained from Miltenyi Biotec (Leiden, the Netherlands), Agilent Technologies (Santa Clara, CA, USA), Beckman Coulter (Brea, CA, USA), and Thermo Fisher Scientific (Waltham, MA, USA), respectively. APC-labeled IgG_1 (clone MOPC-21), FITC-labeled IgG_1 (clone X40) and PE-labeled IgG_1(clone X40) were from BD Biosciences (Franklin Lakes, NJ). For surface plasmon resonance imaging (SPRi) analysis, antibodies against CD8 (clone RPA-T8), CD19 (clone SJ25C1) and CD56 (clone HD56) were purchased at BioLegend (San Diego, CA, USA). Antibodies against CD24 (clone SN3), CD146 (clone P1H12) and PSGL-1 (clone KPL-1) were obtained from eBioscience. Anti-CD61 (clone V1-PL2) and anti-CD66b (clone 80H3) antibodies were from BD Biosciences and GeneTex (Irvine, CA, USA), respectively. For immune-depletion analysis, the CD24 MicroBead Kit from Miltenyi Biotec was used. This kit includes a biotinylated monoclonal antibody against CD24 (clone 32D12) and MicroBeads conjugated with monoclonal anti-biotin antibodies. For fibrin generation, essentially a plasma recalcification assay, the inhibitory antibodies against human (coagulation) FVIIa (clone CLB VII-1) and FXIIa (clone CLB OT2) [24] were obtained from Sanquin (Amsterdam, the Netherlands). For transmission electron microscopical analysis, anti-TF (clone HTF-1) and anti-CD24 (clone SN3) antibodies were obtained from eBioscience and Bio-rad (Hercules, CA, USA), respectively. Rabbit-anti-mouse (RAM) antibody (Agilent Technologies) and colloidal gold particles conjugated to protein A (Utrecht University) were used for detection of the antibodies. For whole blood flow chamber model analysis, the inhibitory antibody against human CD24 (clone SWA11) was described before [17] and an antibody against human CD11b (clone M1/70; Santa Cruz, San Diego, CA, USA) was used as control antibody.

Collection of human saliva

Saliva was collected from healthy human volunteers ($n = 5$) with informed consent after overnight fasting as described previously [2]. Briefly, saliva was collected and centrifuged at $400 \times g$ and 4 °C for 10 min to remove cells. The cell-free supernatant was collected and centrifuged at $1550 \times g$ and 4 °C for 20 min to remove remaining cells and cell debris. The cell-free saliva samples were kept on ice until use.

Flow cytometry analysis of salivary EVs

Salivary EVs were diluted in phosphate buffered saline (PBS) containing citrate (citrate-PBS, 1:10 v/v, pH 7.4; 0.22 μm filtered) to a final concentration of 1.6×10^6 particles/mL to circumvent swarm detection. Before labeling, the antibodies were centrifuged at $18\,900 \times g$ for 5 min at 4 °C to remove aggregates. To identify the cellular origin or to obtain information on the biochemical composition of EVs, 20 μL diluted EVs were incubated with 2.5 μL antibodies of interest. Final concentrations used were: 2.5 μg mL^{-1} for CD8-PE, CD19-PE, CD61-APC and CD146-PE antibodies; and 5 μg mL^{-1} for CD24-FITC, CD56-APC and CD66b-FITC antibodies. APC/FITC/PE-conjugated mouse IgG1 κ isotype antibodies were used as controls (final concentration 2.5 μg mL^{-1} for IgG1-PE and 5 μg mL^{-1} for IgG1-APC and IgG1-FITC). After addition of antibodies, EV-containing samples were incubated in the dark for 2 h at 20 °C. Subsequently, the labeling was stopped by addition of 200 μL citrate-PBS buffer followed by detection of EVs using an Apogee A60 Micro Flow Cytometer

(Apogee Flow Systems, Northwood, UK). Samples were analyzed for 1 min with a flow rate of 3.01 μL min^{-1}. The trigger was set on large angle light scattering (LALS) at 14 and the voltages for 405-small angle light scatter (SALS), 405-LALS, 638-D Red, 488-Green and 488-Orange were set at 380, 375, 510, 520 and 520, respectively. Data were analyzed with the software FlowJo (Version 10, FlowJo LLC, Ashland, OR, USA). Gates were based on isotype controls and the molecules of equivalent soluble fluorescence were calculated as described before [25]. Our flow cytometer detects single EVs, when corrected for refractive index and optical configuration of the instrument, of ~170 nm and larger [26].

Surface plasmon resonance imaging (SPRi) analysis of salivary EVs

The presence of antigens on salivary EVs was studied by SPRi as described previously [25]. In short, antibodies against CD8, CD19, CD24-FITC, CD56, CD61, CD66b, CD146 and PSGL1 were printed on an SPRi sensor (Easy2Spot G-type, Ssens, Enschede, the Netherlands) with a microfluidic printer (CFM 2.0, Wasatch Microfluidics, Salt Lake City, UT, USA). Antibodies were prediluted to 10 μg mL^{-1} in acetic acid buffer (pH 4.5, Merck, Darmstadt, Germany) supplemented with 0.05% (v/v) Tween 80 (Sigma Aldrich, St. Louis, MO, USA) and printed in four spots per antibody. Subsequent blocking was performed with 100 mM 2-amino ethanol followed by 1% (v/v) bovine serum albumin (BSA; both Sigma Aldrich). Unbound material was removed by incubating for 20 min with 0.1 M glycin-HCl (pH 3.0, both Merck) supplemented with 0.3% Triton-X100 (Sigma Aldrich). Saliva was diluted 1 : 1 with PBS (pH 7.4; 0.22 μm filtered) and incubated for 60 min on the sensor surface and material capture was monitored in real time with the MX96 SPRi device (IBIS Technologies, Enschede, the Netherlands). SPRi signals were determined for every antibody spot, compared with surrounding regions without antibodies, and subsequently averaged over the four spots per antibody using home-made software in Matlab R2016b (Mathworks, Natick, MA, USA).

Immune depletion of $CD24^+$ extracellular vesicles from human saliva

The μ Column (Miltenyi Biotec, Leiden, the Netherlands) was prepared according to the manufacturer's description. In general, the μ Column was placed on a magnetic stand and washed once with 100 μL 70% ethanol, followed by three times with 500 μL PBS (pH 7.4; 0.22-μm filtered). Prior to the immune depletion, the concentration of $CD24^+$ EVs was measured by flow cytometry. To circumvent overloading of the column, saliva was diluted with PBS until a concentration of approximately 10^7 mL^{-1} $CD24^+$ EVs was reached. Then, 20 μL biotin-conjugated anti-CD24 antibody was added to the 100 μL diluted saliva sample. The mixture was incubated at 4 °C for 2 h while gently mixing as described, followed by addition of 60 μL PBS buffer and 40 μL monoclonal anti-biotin antibody conjugated Micro Beads, so that the final volume of the mixture was 220 μL (i.e. 2.2-fold diluted compared with the initial saliva sample). The mixture was further incubated at 4 °C for 15 min while gently mixing. After incubation, the mixture was carefully loaded on to the prepared μ Columns without introducing any air bubbles. The flow-through was collected and marked as '$CD24^-$ fraction'. The column was then washed once with 500 μL PBS. The effluent was collected and marked as 'wash'. The column was removed from the magnetic stand, all the remaining contents were flushed from the column with 100 μL PBS by a plunger and marked as '$CD24^+$ fraction'. To correct for the dilution of the initial saliva sample, the '$CD24^+$ fraction' samples were diluted 2.2 times with PBS and all samples were kept on ice until further use.

Measuring the coagulant activity of extracellular vesicles

The fibrin generation assay was performed to determine the coagulant activity of salivary EVs as described previously [2]. In brief, EV-depleted plasma was prepared by centrifuging human pool plasma at 18 900 × *g* and 20 °C for 1 h. For the assay, 70 μL EV-depleted plasma was mixed and incubated with 20 μL indicated sample with or without 6 μL antibodies against FVIIa or FXIIa (final concentration 54 μg mL^{-1}) for 5 min at 37 °C in a 96-well plate. The clotting was initiated by addition of 15 μL $CaCl_2$ (final concentration 13.5 mM) solution. Fibrin generation was monitored by measuring the optical density of the plasma at λ = 405 nm using a SpectraMax i3 microplate detector (Molecular Devices, Sunnyvale, CA, USA) for 1 h at 37 °C. The clotting times (CTs) were defined as described previously [2].

Immunogold label transmission electron microscopy

Salivary EVs were isolated by size-exclusion chromatography (SEC) prior to being immunogold labeled followed by transmission electron microscopic (TEM) analysis. Size-exclusion columns were prepared as described previously [27] with slight modifications. A 15 mL-SPE Flash Column with polyethylene frits (Kinesis, Saint Neots, UK) at both ends was stacked with 10 mL Sepharose CL-2B (GE Healthcare, Chicago, IL, USA), washed in PBS (pH 7.4; 0.22-μm filtered). On each column, 1 mL cell-free saliva was loaded and eluted by PBS. Fractions of 0.5 mL were collected; fractions 8 and 9, which contain most EVs and the lowest concentration of soluble proteins, were pooled for analysis by TEM. SEC-isolated salivary EVs were fixed for 1 h by adding an equal volume of 0.2% paraformaldehyde (Aurion, Wageningen,

the Netherlands) in PBS (pH 7.4; 0.22-μm filtered). EVs were adsorbed on grids by letting formvar-carbon-coated grids float on 10-μL suspensions on a sheet of parafilm for 7 min. Grids were washed three times for 2 min with filtered PBS by transferring the grids from one drop of PBS to another. Grids were incubated with filtered glycine (50 mM in PBS) for 15 min, washed three times, and blocked with Aurion blocking solution (Aurion, Wageningen, the Netherlands) for 30 min. Subsequently, the grids were washed with 0.1% BSA-c™ washing buffer (weight/volume; Aurion), and incubated with the first anti-TF antibody (10 μg mL^{-1}; clone HTF-1; eBioscience) or anti-CD24 (1 μg/mL; clone SN3; Bio-Rad) for 45 min. Grids were washed three times with 0.1% BSA-c™ buffer and incubated for 20 min in the same buffer with rabbit-anti-mouse antibody (17.5 mg/mL; Agilent Technologies). Grids were then washed three times with 0.1% BSA-c™ buffer and incubated with 10 μL protein A conjugated with colloidal gold particles (Utrecht University; 5 nm for CD24 and 10 nm for TF) for 20 min. The grids were washed six times and fixed by incubating for 5 min with 1% glutaraldehyde (Electron Microscopy Sciences, Hatfield, PA, USA) in filtered PBS. For double-labeling, grids were washed another six times and the immunogold staining procedure was repeated from the incubation with filtered 50 mM glycine for 15 min onwards. Instead of anti-TF antibody, grids were subsequently incubated with the second anti-CD24 antibody and 5 nm gold. Finally, the grids were washed in PBS and incubated with 1.75% uranyl acetate (Merck, Darmstadt, Germany) for 7 min and the excess uranyl acetate was blotted on a filter paper and thereafter left to dry. Stained vesicles on grids were visualized with electron microscopy operated at 80 kV (FEI, Thermo Fisher Scientific) using a Veleta 2000 × 2000 side-mounted CCD camera and Imaging Solutions software (Olympus, Tokyo, Japan).

Biological activity test of $TF^+/CD24^+$ salivary EVs in a whole blood flow chamber model

PPACK-PENTA blood of healthy volunteers was collected with approval of the local medical ethical committee of the University Medical Center Utrecht. Glass coverslips and the perfusion chamber were prepared as described before [28] with slight modifications. Glass coverslips were coated with Horm collagen, as previously described [29], for 1.5 h at room temperature and blocked with 1% human serum albumin overnight at 4 °C. PPACK-PENTA blood (includes 10% saline, final concentrations of 50 μM and 20 μg mL^{-1} for PPACK and PENTA, respectively) was perfused using a syringe pump (Harvard Apparatus, Holliston, MA, USA) at a shear rate of 1600 s^{-1} for 3 min. Thereafter, 1 mL human saliva or indicated sample was perfused over the coverslip manually within 1 min, followed by rinsing the coverslip with 1 mL HEPES-Tyrode's buffer (pH 7.4). For indicated samples, 'EV-depleted saliva' was prepared by ultracentrifugation of saliva at 150 000 × *g* and 4 °C for 1 h. 'Saliva + anti-CD24' was prepared by incubating human saliva with an inhibitory anti-CD24 antibody (clone SWA11; final concentration 50 μg mL^{-1}) at 37 °C for 20 min. 'Saliva + antibody control' was prepared by incubating human saliva with an anti-CD11b antibody (clone M1/70; final concentration 50 μg mL^{-1}) at 37 °C for 20 min. Finally, 1 mL recalcified citrated pool plasma ($CaCl_2$ final concentration 9 mM) depleted from endogenous EVs by ultracentrifugation and supplemented with 90 μM Alexa488-conjugated active-site inhibited tissue plasminogen activator (tPA-Alexa488) were co-perfused on the same slip to monitor fibrin generation. In brief, tPA-Alexa488 was prepared by incubating 350 nmol tPA (Boehringer Ingelheim, Ingelheim, Germany) with 35 nmol biotin-labeled PPACK for activity elimination (Haematologic Technologies Inc, Essex Junction, VT, USA) for 1 h at room temperature. Residue tPA not bound to PPACK-biotin inhibitor was removed by dialysis. tPA-PPACK-biotin conjugates were desalted with a ZEBA 5 mL column using HEPES-Tyrode's buffer (pH 7.4), and subsequently mixed with alexa488-conjugated streptavidin and stored at −80 °C until use. Fibrin mesh formation was visualized with an inverted microscope (Zeiss observer Z.1, Carl Zeiss, Sliedrecht, the Netherlands). Videos and snapshots were recorded with differential interference contract (DIC) and Alexa488 (FITC) channels simultaneously, using a 40 x/1.25 oil EC-plan Neofluar objective (Carl Zeiss). All images were analyzed with ZEN2 software (Blue edition, Version 2.0.0.0, Carl Zeiss).

Statistics

Data were analyzed by two-tailed Student's *t*-test (GraphPad Prism software Version 7.0, GraphPad Software, CA, USA). $P < 0.05$ was considered to be statistically significant.

Results

Surface antigens of salivary EVs

EVs were labeled with antibodies against CD8 for T cells, CD19 for B cells, CD56 for natural killer cells, CD61 for platelets, CD66b for granulocytes, CD146 for endothelial cells, and CD24 and PSGL-1 as ligands of P-selectin. CD24 and CD66b stained the highest numbers of salivary EVs as detected by flow cytometry (Fig. 1). To confirm the flow cytometry results, we also studied the exposure of CD24, CD66b and PSGL-1 by SPRi [25]. The SPRi results shown in Fig. 2 confirm that CD24 and CD66b are clearly present on salivary EVs, whereas PSGL-1 is either absent or below the limit of detection.

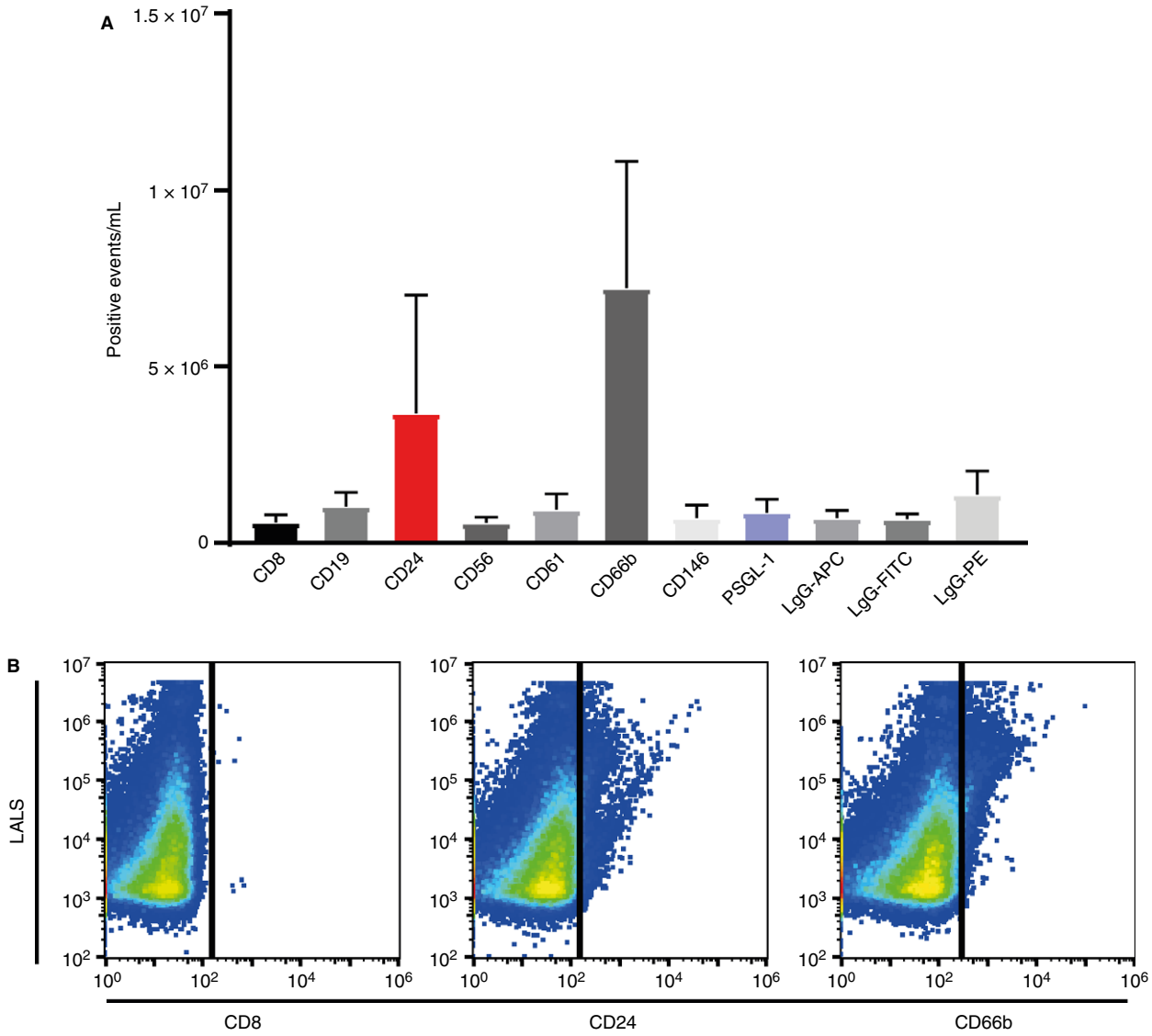

Fig. 1. (A) Flow cytometry analysis of salivary extracellular vesicles (EVs). Data are shown as mean ± SD (n = 5 healthy controls). (B) Representative dot-plots of salivary EVs labeled with antibodies against CD8, CD24 and CD66b. [Color figure can be viewed at wileyonlinelibrary.com]

Occurrence of CD24 and TF on salivary EVs

We hypothesized that CD24 is involved in delivery of coagulant TF to a site of vascular injury. Therefore, we determined whether CD24 and coagulant TF co-localize on salivary EVs. Saliva samples were immune-depleted using CD24 antibody-coated beads (Fig. 3A). The flow through (i.e. the $CD24^-$ fraction) and the fraction containing the $CD24^+$ EVs were collected separately to study their coagulant activity. Firstly, we showed that the coagulant activity of human saliva is exclusively associated with EVs (Fig. 3B), and salivary EVs trigger clotting faster than EVs isolated from LPS-stimulated human whole blood ($P < 0.05$; Figure S1). Secondly, the TF coagulant activity of the cell-free saliva was abolished after capturing CD24-exposing EVs (Fig. 3C, $CD24^-$ fraction). In contrast, the fraction containing the captured CD24-exposing EVs promoted TF-dependent fibrin formation, which was completely inhibited by an antibody against human FVIIa but insensitive to inhibition of FXIIa (Fig. 3D–E). Thus, we deduce that CD24 and coagulant TF co-localize on a subpopulation of salivary EVs. We further investigated the cellular origin of the $CD24^+$ EVs by flow cytometry, by double-labeling the EVs with anti-CD66b, a granulocyte marker (Fig. 3F). More than 70% of the $CD24^+$ EVs double-stained for CD66b, suggesting that most of the CD24-exposing EVs originate from granulocytes (Fig. 3G). The coagulant activity of saliva was strongly inhibited by immune depletion of $CD66b^+$ EVs, confirming that coagulant TF-EVs in human saliva are likely to originate from granulocytes (n = 5, Figure S2).

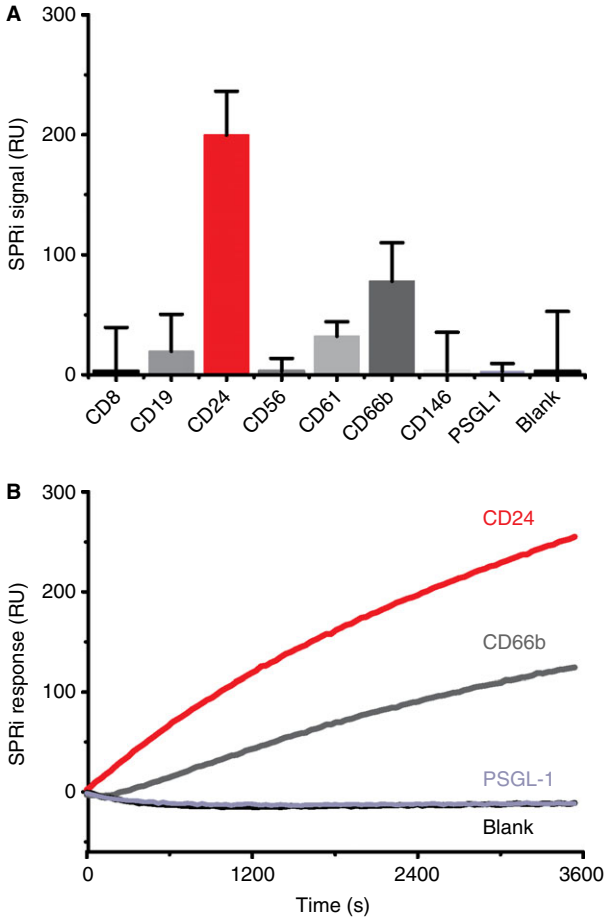

Fig. 2. (A) Detection of antigens on salivary extracellular vesicles (EVs) by surface plasmon resonance imaging (SPRi). SPRi signals were obtained after 1 h of incubation with salivary EVs. Data are presented as mean ± SD (n = 4). (B) Representative SPRi sensorgram showing the binding curves of salivary EVs to (anti) PSGL-1, CD24, CD66b and blank.[Color figure can be viewed at wileyonlinelibrary.com]

To confirm that CD24 and TF indeed co-exist, we performed immunogold labeling after isolation of EVs by SEC (Fig. 4). Salivary EVs were labeled with anti-TF antibody tagged with 10 nm gold particles (Fig. 4A, black arrows), anti-CD24 antibody tagged with 5 nm gold particles (Fig. 4B, white arrows), or both (Fig. 4C, i–iv) and controls (Fig. 4D–G). As illustrated in Fig. 4(C, i–iv), both CD24 and TF were observed on a subpopulation of salivary EVs. When evaluating 200 EVs, 28% stained for both CD24 and TF, 20% for CD24, 9% for TF and 43% were negative for both CD24 and TF. In summary, electron microscopy confirms that a subpopulation of salivary EVs expose both TF and CD24.

Salivary EVs deposit coagulant tissue factor on platelets via CD24

We next investigated whether the $CD24^+/TF^+$ human salivary EVs are being deposited at the surface of activated platelets and trigger coagulation in a whole blood perfusion model. Blood was perfused over collagen-coated cover slips for 3 min (Fig. 5A, a). During perfusion, platelets adhered to collagen, underwent morphological changes suggesting platelet activation and formed aggregates (Fig. 5A, b). Thereafter, saliva containing EVs or indicated samples was perfused, followed by washing with buffer to remove unbound components (Fig. 5A, c). Because of the diffraction limit, the deposition of salivary EVs on platelets cannot be observed directly and therefore no differences were detectable between Fig. 5(A, b) and 5(A, c) Finally, plasma was mixed with FITC-conjugated tPA and perfused to monitor fibrin generation in time (Fig. 5A, d). Within 2 min a fibrin network was formed starting at the site of platelet aggregates when the plasma was perfused over the sample that had been pretreated with EV-containing saliva (Fig. 5B, average = 111 s; Video S2.1). In contrast, no fibrin formation was observed within 15 min when the plasma was perfused over the EV-depleted saliva (Video S2.2). When plasma was perfused over the sample pretreated with EV-containing saliva in the presence of anti-CD24, the time to fibrin formation increased to over 700 s (Fig. 5B, Video S2.3). In contrast, the time of fibrin formation was unaffected when the plasma was perfused over EV-containing saliva that had been pretreated with a control antibody (Video S2.4). Thus, blocking CD24 on salivary EVs inhibits the deposition of TF on platelet aggregates under flow conditions.

Discussion

Previously, the interaction between CD24 and P-selectin has been studied extensively in both human and mice models using transfected cell lines, inhibitory antibodies and binding assays [17, 30–33]. In addition to these static interaction studies, the interaction between CD24 and P-selectin was shown to support rolling of breast cancer cells on endothelial cells in a flow model [18]. In our study, we demonstrate that EVs from human saliva expose CD24, a ligand of P-selectin, as well as TF, and that these EVs are deposited on activated platelets, where they trigger TF-dependent coagulation. Although a role of P-selectin seems likely, we were unable to purchase or obtain an inhibitory antibody against P-selectin, and therefore the role of P-selectin needs to be confirmed.

Regarding the cellular origin of the $CD24^+$ EVs, saliva of healthy human individuals is known to contain granulocytes [34,35]. When we labeled cells in saliva with anti-CD66b, a major cell population stained for this granulocyte marker (Figure S3A–C). Furthermore, most granulocytes were also double-labeled with anti-CD24 (Figure S3D). Next, we studied whether granulocytes release EVs in a whole blood model (Figure S3E–H). In response to LPS, granulocytes released $CD66b^+/CD24^+$ EVs, thus confirming that granulocytes release EVs exposing CD24.

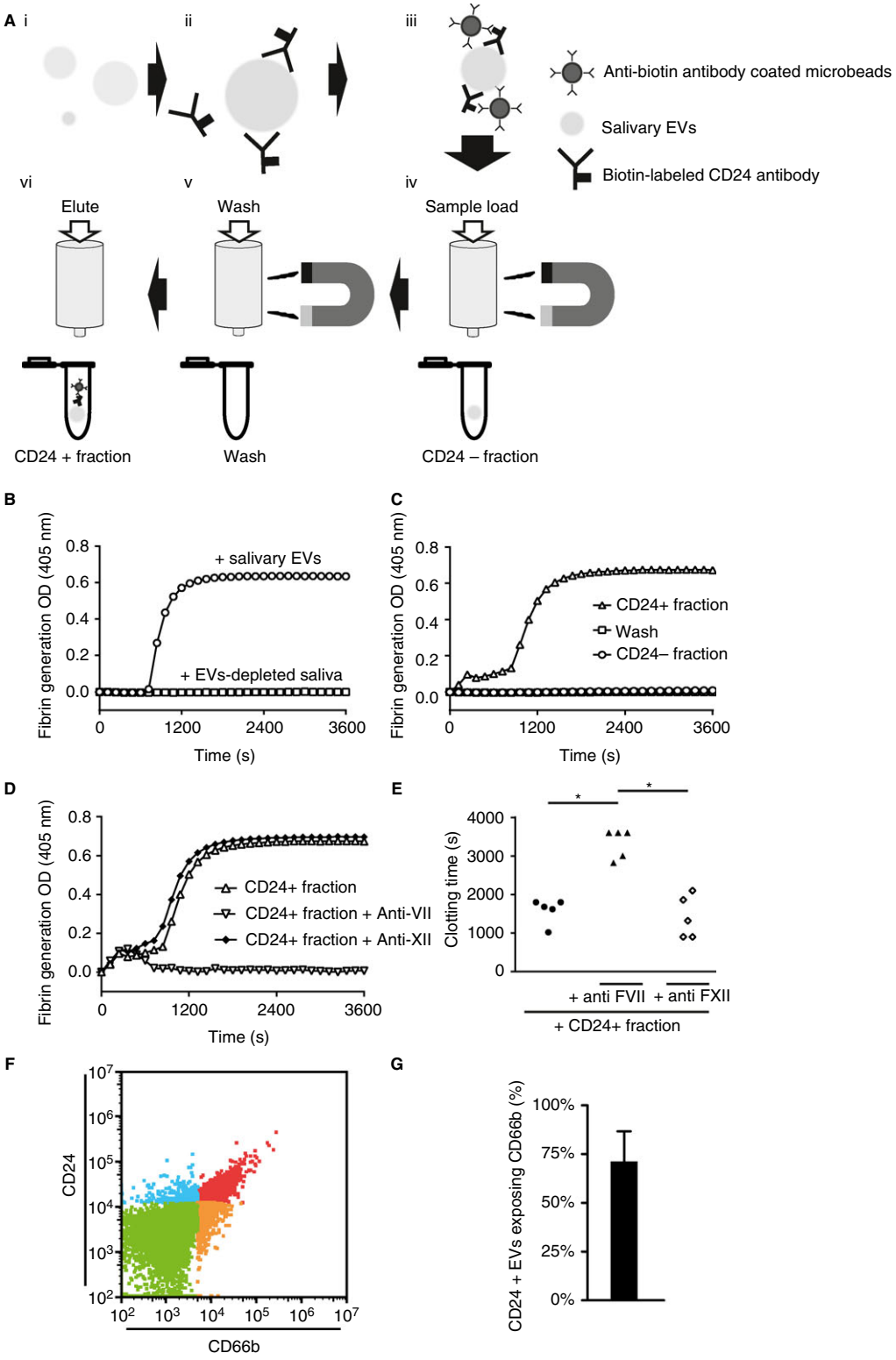

Fig. 3. Immune depletion of CD24-exposing extracellular vesicles (EVs) from human saliva. Salivary EVs were immune depleted using a magnetic column with CD24-biotin conjugated antibody and anti-biotin-coated microbeads. (A) Schematic diagram of the immune-depletion experiments. (B) Human salivary EVs trigger the clotting of plasma. (C) Immune-depleting $CD24^+$ fraction abolishes the clotting triggered by saliva. (D, E) $CD24^+$ salivary EVs trigger coagulation, which is mediated by factor VIIa but independent of factor XIIa. (F) Representative dot-plot of salivary EVs double-labeled with antibodies against CD24 and CD66b. (G) Percentage of CD24-exposing salivary EVs also exposing CD66b, a granulocyte marker ($n = 5$); $^*P < 0.05$. For the negative control, we also performed immune depletion with CD11b, which was ineffective (data not shown). [Color figure can be viewed at wileyonlinelibrary.com]

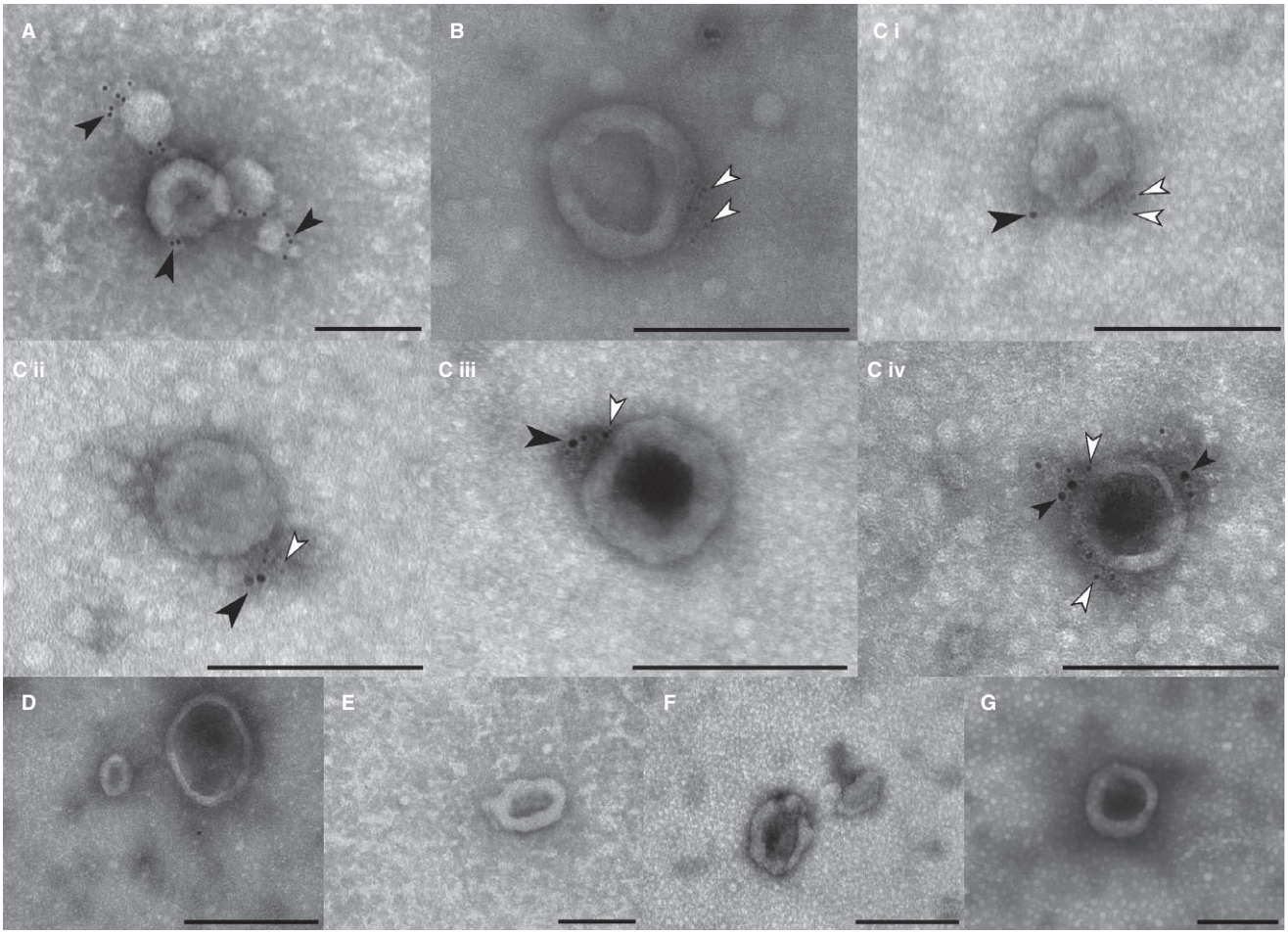

Fig. 4. Immunogold labeling of extracellular vesicles (EVs) from human saliva. A subpopulation of salivary EVs expose both CD24 and tissue factor (TF), indicated by black and white arrows, respectively. Representative transmission electron microscopic (TEM) images of salivary EVs stained with anti-TF antibody tagged with 10-nm gold particles (A), anti-CD24 antibody tagged with 5-nm gold particles (B), or both (Ci–iv). Representative controls of vesicles labeled with control antibody (IgG) plus protein A gold staining (D), no antibody and immunogold labeling with 5 nm gold (E) or 10 nm (F) or with two sizes (5 nm and 10 nm, G). All scale bars represent 200 nm.

The diameter of EVs stained for TF and CD24 are mostly 200 nm and larger, as shown by TEM. In suspension, the diameter of EVs will be slightly larger because EVs shrink to dehydration and fixation by about 14% when being prepared for TEM [26]. Therefore, a major fraction of the single EVs staining for TF and/or CD24 is indeed above the detection limit and thus can be measured by our flow cytometer. Both ultracentrifugation and passing cell-free saliva through a 0.2-μM filter reduced the number of EVs measured by flow cytometry when labeled with anti-CD24 antibody or lactadherin (data not shown), confirming the presence of such EVs in saliva. We assume that the size distribution of salivary particles as detected by tunable resistive pulse sensing (Figure S4) reflects mostly non-EV particles, as previously shown for human plasma [36].

The function of TF-exposing EVs has been extensively studied in *vitro* as well as *in vivo* [15,37–40]. Tumor-derived TF-exposing EVs induce platelet aggregation [15,41] and enhance the size of venous clots in mice [38]. Previous studies have shown that tumor-derived EVs increase the size of venous clots by delivering coagulant TF via PSGL-1, which interacts with P-selectin on activated platelets [15,16,39]. A recent study showed that TF^+ EVs from the human pancreatic cancer cell line BxPc-3 increased venous thrombosis in a mice model. Because these EVs exposed CD24 but not PSGL-1[38], CD24 may be responsible for delivery of coagulant TF to the site of vascular damage, thus contributing to hemostasis on the one hand, but possibly also increasing the risk of developing venous thrombosis. However, whether $CD24^+$ TF-exposing EVs occur in pancreatic cancer patients, and whether such EVs play a role in increasing the incidence of venous thrombosis in cancer patients, needs further investigation. In reality, it is likely that not one but a set of receptors and ligands are involved in the interactions between circulating EVs and an area of vascular damage. Indeed, for a different pancreatic cell line, Panc02, Thomas *et al*. showed that the clot size in a mice stenosis model is independent of P-selectin [37] but

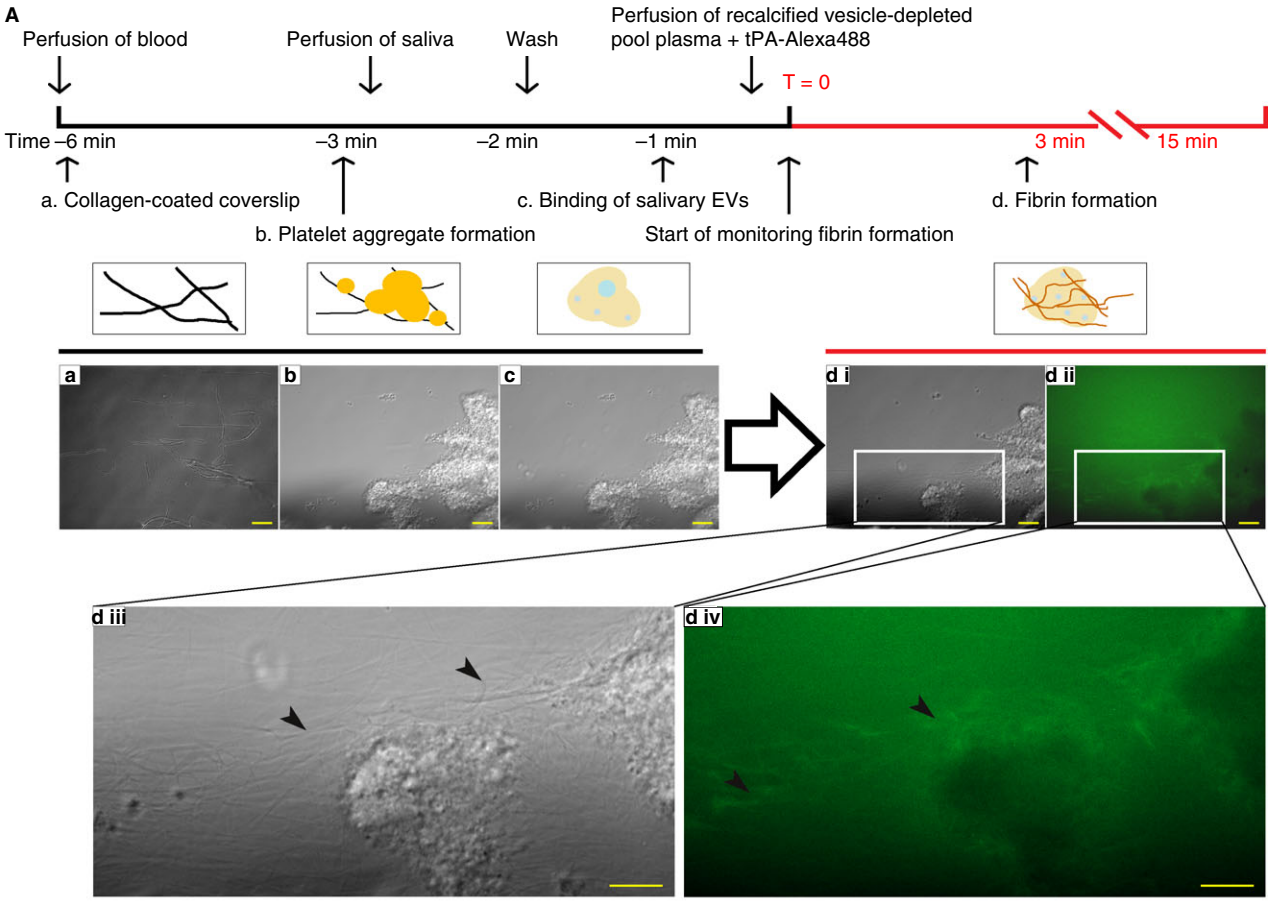

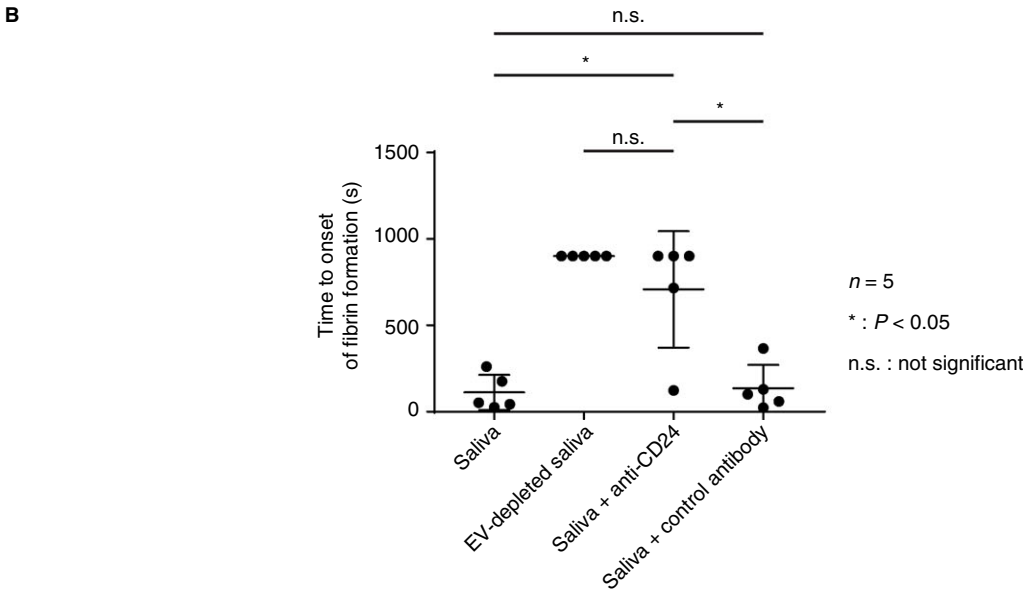

Fig. 5. Binding of salivary extracellular vesicles (EVs) to activated platelets under flow conditions. (A) Schematic overview of the perfusion experiments: (a) collagen (type I and III) was used to coat the coverslip of the chamber, imitating an open wound; (b) platelet aggregates formed after whole blood perfusion; (c) perfusion of saliva; (d i) bright field picture of fibrin formation; (d ii) fluorescent image of fibrin formation taken immediately (approximately 1 s) after picture d I; (d iii) enlarged picture of d I; (d iv) enlarged picture of d ii. All scale bars represent 20 μm and fibrin strains are indicated by black arrows in diii and div. (B) Time to onset (T = 0) of fibrin formation after plasma perfusion. Fibrin formation starting at the platelet aggregates was observed after about 2 min for the sample that had been perfused with EV-containing saliva, whereas no fibrin formation was observed within 15 min in the sample that was perfused with the EV-depleted saliva. Pretreatment of the saliva with anti-CD24 greatly delayed the onset of fibrin formation to over 700 s. [Color figure can be viewed at wileyonlinelibrary.com]

mediated by $\alpha_v\beta_1$ and/or $\alpha_v\beta_3$ [42]. Because there are many differences between the before mentioned studies, including differences in the origin and composition of EVs, it seems likely that various receptors may play a role in different thrombosis models.

In sum, our present study shows for the first time that coagulant TF, exposed on $CD24^+$ EVs in human saliva of healthy individuals, can be delivered at a site of vascular injury. In addition, our findings indicate that the deposited EVs trigger coagulation and thus facilitate an efficient hemostasis, thereby reducing the risk of infection and explaining our reflex of licking a wound.

Addendum

Y. Yu and R. Nieuwland designed the research; Y. Yu, E. Gool and A. D. Barendrecht performed the experiments; Y. Yu, E. Gool, R. J. Berckmans, A. D. Barendrecht, C. Maas, N. N. van der Wel, A. Sturk and R. Nieuwland analyzed and interpreted the data; Y. Yu drafted the manuscript; E. Gool, R. J. Berckmans, A. D. Barendrecht, C. Maas, N. N. van der Wel, P. Altevogt, F. A. W. Coumans, A. Sturk and R. Nieuwland participated in manuscript preparation. All authors reviewed the manuscript.

Acknowledgements

The authors thank A. E. Grootemaat (Department of Medical Biology, Electron Microscopy Centre Amsterdam, AMC, Amsterdam, the Netherlands) and C. C. Clark (Department of Clinical Chemistry and Haematology, University Medical Center Utrecht, Utrecht, the Netherlands) for their technical assistance. We acknowledge funding from the Netherlands organization for scientific research-domain applied and engineering sciences, programs Veni B681 (F. A. W. Coumans) and STW perspectief Cancer ID 14195 (E. Gool).

Disclosure of Conflict of Interests

F. A. W. Coumans reports grants from NWO-TTW VENI 13681 during the conduct of the study. E. Gool reports grants from NWO Applied and Engineering Sciences during the conduct of the study. The other authors state that they have no conflict of interest.

Supporting Information

Additional supporting information may be found online in the Supporting Information section at the end of the article:

Fig. S1. Plasma clotting induced by salivary EVs versus LPS-stimulated human whole blood-derived EVs. Whole blood was stimulated with LPS, then the EVs were collected by removal of the cells and the EV-containing plasma were tested undiluted or with 2, 5 and 10-fold dilution. The plasma clotting time induced by the salivary EVs was much shorter than the undiluted LPS-stimulated blood EVs.

Fig. S2. Clotting time of human plasma induced by $CD24^+$ and $CD66b^+$ salivary EVs in the absence or presence of the inhibitory antibody against human factor VIIa ($n = 5$)

Fig. S3. Representative dot-plots of salivary cells labeled with control antibody (A) or anti-CD66b (B), overlay of control antibody and anti-CD66b (C) and double-labeling with CD66b and CD24 (D). Representative dot-plots of LPS-stimulated human whole blood-derived EVs labeled with anti-CD24 (E), CD66b (F), CD66b and CD24 (G); percentage of $CD24^+$ EVs exposing $CD66b^+$ (H, $n = 4$).

Fig. S4. Size distribution of salivary EVs measured by tunable resistive pulse sensing. The red line at 70 nm indicates the lower limit of tunable resistive pulse sensing detection.

Video S1.1. Monitoring of fibrin formation on saliva-perfused platelet aggregates.

Video S1. 2. Monitoring of fibrin formation on EV-depleted saliva-perfused platelet aggregates.

Video S1. 3. Monitoring of fibrin formation on CD24 neutralized-saliva-perfused platelet aggregates.

Video S1. 4. Monitoring of fibrin formation on IgG control-incubated saliva-perfused platelet aggregates.

References

1 Geddings JE, Mackman N. Tumor-derived tissue factor-positive microparticles and venous thrombosis in cancer patients. *Blood* 2013; **122**: 1873–80.
2 Berckmans RJ, Sturk A, van Tienen LM, Schaap MCL, Nieuwland R. Cell-derived vesicles exposing coagulant tissue factor in saliva. *Blood* 2011; **117**: 3172–80.
3 Kouwaki T, Okamoto M, Tsukamoto H, Fukushima Y, Oshiumi H. Extracellular vesicles deliver host and virus RNA and regulate innate immune response. *Int J Mol Sci* 2017; **18**: 666.
4 Shigemoto-Kuroda T, Oh JY, Kim DK, Jeong HJ, Park SY, Lee HJ, Park JW, Kim TW, An SY, Prockop DJ, Lee RH. MSC-derived extracellular vesicles attenuate immune responses in two autoimmune murine models: type 1 diabetes and uveoretinitis. *Stem Cell Rep* 2017; **8**: 1214–25.
5 Hoshino A, Costa-Silva B, Shen TL, Rodrigues G, Hashimoto A, Mark MT, Molina H, Kohsaka S, Di Giannatale A, Ceder S, Singh S, Williams C, Soplop N, Uryu K, Pharmer L, King T, Bojmar L, Davies AE, Ararso Y, Zhang T, *et al*. Tumour exosome integrins determine organotropic metastasis. *Nature* 2015; **527**: 329–35.
6 Kaplan RN, Rafii S, Lyden D. Preparing the "soil": the premetastatic niche. *Cancer Res* 2006; **66**: 11089–93.
7 Berezin AE, Kremzer AA, Samura TA, Martovitskaya YV, Malinovskiy YV, Oleshko SV, Berezina TA. Predictive value of apoptotic microparticles to mononuclear progenitor cells ratio in advanced chronic heart failure patients. *J Cardiol* 2015; **65**: 403–11.
8 Zwicker JI. Predictive value of tissue factor bearing microparticles in cancer associated thrombosis. *Thromb Res* 2010; **125** (Suppl 2): S89–91.
9 Biro E, Sturk-Maquelin KN, Vogel GMT, Meuleman DG, Smit MJ, Hack CE, Sturk A, Nieuwland R. Human cell-derived microparticles promote thrombus formation in vivo in a tissue factor-dependent manner. *J Thromb Haemost* 2003; **1**: 2561–8.

10 Nieuwland R, Berckmans RJ, RotteveelEijkman RC, Maquelin KN, Roozendaal KJ, Jansen PGM, tenHave K, Eijsman L, Hack CE, Sturk A. Cell-derived microparticles generated in patients during cardiopulmonary bypass are highly procoagulant. *Circulation* 1997; **96**: 3534–41.
11 Callander NS, Varki N, Rao LV. Immunohistochemical identification of tissue factor in solid tumors. *Cancer* 1992; **70**: 1194–201.
12 Rak J, Milsom C, Yu J. Tissue factor in cancer. *Curr Opin Hematol* 2008; **15**: 522–8.
13 Davila M, Amirkhosravi A, Coll E, Desai H, Robles L, Colon J, Baker CH, Francis JL. Tissue factor-bearing microparticles derived from tumor cells: impact on coagulation activation. *J Thromb Haemost* 2008; **6**: 1517–24.
14 Mackman N. New insights into the mechanisms of venous thrombosis. *J Clin Invest* 2012; **122**: 3368.
15 Thomas GM, Panicot-Dubois L, Lacroix R, Dignat-George F, Lombardo D, Dubois C. Cancer cell-derived microparticles bearing P-selectin glycoprotein ligand 1 accelerate thrombus formation in vivo. *J Exp Med* 2009; **206**: 1913–27.
16 Falati S, Liu QD, Gross P, Merrill-Skoloff G, Chou J, Vandendries E, Celi A, Croce K, Furie BC, Furie B. Accumulation of tissue factor into developing thrombi in vivo is dependent upon microparticle P-selectin glycoprotein ligand 1 and platelet P-selectin. *J Exp Med* 2003; **197**: 1585–98.
17 Aigner S, Sthoeger ZM, Fogel M, Weber E, Zarn J, Ruppert M, Zeller Y, Vestweber D, Stahel R, Sammar M, Altevogt P. CD24, a mucin-type glycoprotein, is a ligand for P-selectin on human tumor cells. *Blood* 1997; **89**: 3385–95.
18 Aigner S, Ramos CL, Hafezi-Moghadam A, Lawrence MB, Friederichs J, Altevogt P, Ley K. CD24 mediates rolling of breast carcinoma cells on P-selectin. *Faseb J* 1998; **12**: 1241–51.
19 Springer T, Galfre G, Secher DS, Milstein C. Monoclonal xenogeneic antibodies to murine cell surface antigens: identification of novel leukocyte differentiation antigens. *Eur J Immunol* 1978; **8**: 539–51.
20 Pirruccello SJ, Lebien TW. The human B-cell-associated antigen Cd24 is a single chain sialoglycoprotein. *J Immunol* 1986; **136**: 3779–84.
21 Fischer GF, Majdic O, Gadd S, Knapp W. Signal transduction in lymphocytic and myeloid cells via Cd24, a new member of phosphoinositol-anchored membrane molecules. *J Immunol* 1990; **144**: 638–41.
22 Kay R, Rosten P, Humphries RK. Cd24, a signal transducer modulating B-cell activation responses, is a very short peptide with a glycosyl phosphatidylinositol membrane anchor. *Exp Hematol* 1991; **147**: 1412–6.
23 Williams LA, Hock BD, Hart DNJ. Human T lymphocytes and hematopoietic cell lines express CD24-associated carbohydrate epitopes in the absence of CD24 mRNA or protein. *Blood* 1996; **88**: 3048–55.
24 de Maat S, Bjorkqvist J, Suffritti C, Wiesenekker CP, Nagtegaal W, Koekman A, van Dooremalen S, Pasterkamp G, de Groot PG, Cicardi M, Renne T, Maas C. Plasmin is a natural trigger for bradykinin production in patients with hereditary angioedema with factor XII mutations. *J Allergy Clin Immun* 2016; **138**: 1414–23.
25 Gool EL, Stojanovic I, Schasfoort RBM, Sturk A, van Leeuwen TG, Nieuwland R, Terstappen LWMM, Coumans FAW. Surface plasmon resonance is an analytically sensitive method for antigen profiling of extracellular vesicles. *Clin Chem* 2017; **63**: 1633–41.
26 Van der Pol E, ISTH-SSC-VB Working group, Sturk A, van Leeuwen TG, Nieuwland R, Coumans FA. Standardization of extracellular vesicle measurements by flow cytometry through vesicle diameter approximation. *J Thromb Haemost* 2018; **16**: 1236–45.
27 Boing AN, van der Pol E, Grootemaat AE, Coumans FA, Sturk A, Nieuwland R. Single-step isolation of extracellular vesicles by size-exclusion chromatography. *J Extracell Vesicles* 2014; **3**: https://doi.org/10.3402/jev.v3.23430.
28 Tersteeg C, Heijnen HF, Eckly A, Pasterkamp G, Urbanus RT, Maas C, Hoefer IE, Nieuwland R, Farndale RW, Gachet C, de Groot PG, Roest M. FLow-induced PRotrusions (FLIPRs): a platelet-derived platform for the retrieval of microparticles by monocytes and neutrophils. *Circ Res* 2014; **114**: 780–91.
29 Barendrecht AD, Verhoef JJF, Pignatelli S, Pasterkamp G, Heijnen HFG, Maas C. Live-cell imaging of platelet degranulation and secretion under flow. *J Vis Exp* 2017; **125**: https://doi.org/10.3791/55658.
30 Friederichs J, Zeller Y, Hafezi-Moghadam A, Grone HJ, Ley K, Altevogt P. The CD24/P-selectin binding pathway initiates lung arrest of human A125 adenocarcinoma cells. *Cancer Res* 2000; **60**: 6714–22.
31 Chen C, He Z, Sai P, Faridi A, Aziz A, Kalavar M, Griciene P, Gintautas J, Steier W. Inhibition of human CD24 binding to platelet-bound P-selectin by monoclonal antibody. *Proc West Pharmacol Soc* 2004; **47**: 28–9.
32 Baumann P, Cremers N, Kroese F, Orend G, Chiquet-Ehrismann R, Uede T, Yagita H, Sleeman JP. CD24 expression causes the acquisition of multiple cellular properties associated with tumor growth and metastasis. *Cancer Res* 2005; **65**: 10783–93.
33 Sammar M, Aigner S, Hubbe M, Schirrmacher V, Schachner M, Vestweber D, Altevogt P. Heat-stable antigen (CD24) as ligand for mouse P-selectin. *Int Immunol* 1994; **6**: 1027–36.
34 Gillum T, Kuennen M, McKenna Z, Castillo M, Jordan-Patterson A, Bohnert C. Exercise does not increase salivary lymphocytes, monocytes, or granulocytes, but does increase salivary lysozyme. *J Sport Sci* 2017; **35**: 1294–9.
35 Lakschevitz FS, Glogauer M. High-purity neutrophil isolation from human peripheral blood and saliva for transcriptome analysis. *Methods Mol Biol* 2014; **1124**: 469–83.
36 Buzas EI, Gardiner C, Lee C, Smith ZJ. Single particle analysis: methods for detection of platelet extracellular vesicles in suspension (excluding flow cytometry). *Platelets* 2017; **28**: 249–55.
37 Thomas GM, Brill A, Mezouar S, Crescence L, Gallant M, Dubois C, Wagner DD. Tissue factor expressed by circulating cancer cell-derived microparticles drastically increases the incidence of deep vein thrombosis in mice. *J Thromb Haemost* 2015; **13**: 1310–9.
38 Hisada Y, Ay C, Auriemma AC, Cooley BC, Mackman N. Human pancreatic tumors grown in mice release tissue factor-positive microvesicles that increase venous clot size. *J Thromb Haemost* 2017; **15**: 2208–17.
39 del Conde I, Shrimpton CN, Thiagarajan P, Lopez JA. Tissue-factor-bearing microvesicles arise from lipid rafts and fuse with activated platelets to initiate coagulation. *Blood* 2005; **106**: 1604–11.
40 Cohen JG, Prendergast E, Geddings JE, Walts AE, Agadjanian H, Hisada Y, Karlan BY, Mackman N, Walsh CS. Evaluation of venous thrombosis and tissue factor in epithelial ovarian cancer. *Gynecol Oncol* 2017; **146**: 146–52.
41 Geddings JE, Hisada Y, Boulaftali Y, Getz TM, Whelihan M, Fuentes R, Dee R, Cooley BC, Key NS, Wolberg AS, Bergmeier W, Mackman N. Tissue factor-positive tumor microvesicles activate platelets and enhance thrombosis in mice. *J Thromb Haemost* 2016; **14**: 153–66.
42 Mezouar S, Darbousset R, Dignat-George F, Panicot-Dubois L, Dubois C. Inhibition of platelet activation prevents the P-selectin and integrin-dependent accumulation of cancer cell microparticles and reduces tumor growth and metastasis in vivo. *Int J Cancer* 2015; **136**: 462–75.